IAU-ARAK

J. Iran. Chem. Res. 2 (2009) 277-291

Journal of the Iranian Chemical Research

www.iau-jicr.com

Biologically vital metal-based antimicrobial active mixed ligand complexes: synthesis, characterization, DNA binding and cleavage studies

Natarajan Raman *, Ramaraj Jeyamurugan, Arumhgam Sakthivel, Rajendran Antony

Research Department of Chemistry, VHNSN College, Virudhunagar-626 001, India

Received 1 July 2009; received in revised form 17 October 2009; accepted 20 November 2009

Abstract

Few novel cobalt(II) and copper(II) complexes $[M(fmp)_3]Cl_2$, $[M(fmp)(bpy)_2]Cl_2$, $[M(fmp)(phen)_2]Cl_2$ and $[M(fmp)(phen)(bpy)]Cl_2$ (fmp = 3-furan-2-ylmethylene-pentane-2,4-dione, phen = 1,10-phenanthroline, bpy = 2,2'-bipyridine) have been synthesized and characterized by elemental analyses, molar conductance, magnetic susceptibility measurements, IR, electronic, EPR, mass spectra and cyclic voltammetric studies. The synthesized complexes are found to be monomeric and electrolytic nature. The UV-Vis., magnetic susceptibility and EPR spectral data of the complexes suggest a distorted octahedral geometry for Cu(II) complexes and octahedral geometry for Co(II) complexes around the central metal ion. The CV profile of the complexes shows a quasi-reversible peak which indicates that the metal-ligand linkage is more covalent in nature. Spectroscopic and viscosity measurements prove that the $[M(fmp)(phen)_2]Cl_2$ complexes bind more efficiently with DNA than other complexes through intercalative mode. The difference of peak potential and electrochemical parameters between free and DNA-bound complexes shows the formation of an electrochemical active complex between synthesized complexes and DNA. All the complexes cleave the Supercoiled pUC19 DNA *in vitro* under the presence of reducing agent (3-mercaptopropionic acid). The *in vitro* antimicrobial activities of the compounds have been tested against the bacterial and fungal strains using the disc diffusion method. The minimum inhibitory concentration (MIC) values against the growth of microorganisms are much larger for metal chelates than the individual ligands.

Keywords: β-diketone; Complexes; DNA binding; Oxidative cleavage; Antimicrobial.

1. Introduction

Metal ions coordinated with β-diketones have been widely investigated to their manifestation of novel structural features, unusual magnetic properties and relevance to biological process [1-3]. Over the last few years, the chemistry of β-diketone containing compounds has become an active area of research. Different and interesting behaviour has been observed by substituting these β-diketone ligands with nitrogen containing chelate groups such as 1,10-phenanthroline or 2,2'-bipyridine with transition metal(II) ions [4, 5]. Transition metal complexes are useful as chemical nucleases due to their versatile structure, redox behaviour and physiological properties. The binding and cleavage of DNA using transition metal complexes has

* Corresponding author. Tel.: +91 9245165958, fax: +91 4562 281338.
E-mail address: drn_raman@yahoo.co.in (N. Raman)

received a great deal of attention during the past decade. Mixed ligands having bipyridine and phenanthroline show different property to interact with DNA and also with microbes.

The study of mixed ligand-complex formation is relevant in the field of analytical chemistry, where the use of mixed ligand complexes allows the development of methods with increased selectivity, sensitivity and has also great importance in the field of biological and environmental chemistry [6]. The Knoevenagel condensate, obtained from furfuraldehyde and acetylacetone, has two oxygen donor atoms. It can form six coordinate octahedral complexes when present in 1:3 (metal: ligand) ratio. In 1:1 stoichiometry, the ligand forms two bonds with the metal ion leaving four position to be occupied by the anions or bases to form a six coordinate system requiring octahedral geometry. Among the bidentate nitrogenous bases, those containing the 2,2'-bipyridine ring form metal chelates with exceptional spectroscopic, photophysical and photochemical properties [7-9]. 2,2'-Bipyridine or 1,10-phenanthroline and its derivatives have been receiving considerable attention, largely because of their ability to form coordination compounds with metal ions [10].

There is no work has been done on the mixed ligand of the Knoevenagel condensate obtained from furfuraldehyde and acetylacetone with 2,2'-bipyridine and 1,10-phenanthroline. This tempted us to synthesize few mixed ligand transition metal complexes, especially biologically important copper and cobalt complexes, using the above ligands in different molar ratio and to analyze the DNA binding and cleavage activities with these complexes.

2. Experimental

2.1. Chemicals

All reagents and chemicals were procured from Merck products. Solvents used for electrochemical and spectroscopic studies were purified by standard procedures [11]. CT DNA was purchased from Bangalore Genei (India). DNA solution in Tris-HCl/ NaCl (pH 7.2) buffer medium gave a ratio of A_{260}/ A_{280}, of *ca.* 1.9:1, indicating that the DNA was sufficiently free from protein concentration [12]. Stock solutions were stored at 4 ^{o}C and used within 4 days. Agarose (molecular biology grade), ethidium bromide (EB), tetrabutylammonium perchlorate were obtained from Sigma (USA). Tris–HCl buffer solution was prepared using deionized, sonicated triply distilled water.

2.2. Instrumentation

Elemental analyses (C, H and N) were carried out with a Calrlo Erba 1108 analyzer. IR spectra of the samples were recorded in the region 4000-400 cm^{-1} using KBr pellets and a Perkin–Elmer 783 spectrophotometer. ^{1}H-NMR spectra (300 MHz) of the sample was recorded in $CDCl_3$ by employing TMS as internal standard on a Bruker Avance DRX 300 FT-NMR spectrometer. Fast atomic bombardment mass spectra (FAB-MS) were obtained using a VGZAB-HS spectrometer in a 3-nitrobenzylalcohol matrix. The X-band ESR spectra of the complexes were recorded at RT (300 K) and LNT (77 K) using TCNE (tetracyanoethylene) as the g-marker. Electronic absorption spectra were recorded using a Shimadzu UV-1601 spectrophotometer.

2.3. DNA binding experiments

The DNA binding experiments were carried out in Tris-HCl/ NaCl (pH 7.2) buffer using the copper complex in DMF. The DNA concentration per nucleotide was determined by absorption spectroscopy using the molar absorption coefficient (6600 $M^{-1}cm^{-1}$) at 260 nm [13]. Absorption titration experiments were performed by varying the concentration of the DNA with the

complex. All UV–Vis. spectra were recorded after equilibration. The intrinsic binding constant K_b was determined from a plot of [DNA] / (ε_a-ε_f) *versus* [DNA] equation (1).

$$[DNA] / (\varepsilon_a-\varepsilon_f) = [DNA] / (\varepsilon_a-\varepsilon_f) + 1/ K_b (\varepsilon_b-\varepsilon_f) \quad \text{----------} \quad (1)$$

where ε_a, ε_f and ε_b are the extinction coefficients of apparent, free and bound form of the complex to DNA respectively.

Viscosity experiments were carried on an Ostwald viscometer, immersed in a thermostated water-bath maintained at a constant temperature at 30.0 ± 0.1°C. DNA samples of approximately 0.5 mM were prepared by sonicating in order minimize complexities arising from DNA flexibility [14]. Flow time was measured with a digital stopwatch three times for each sample and an average flow time was calculated. Data were presented as $(\eta/\eta^0)^{1/3}$ *versus* the concentration of the Cu(II) complex, where η is the viscosity of DNA solution in the presence of complex, and η^0 is the viscosity of DNA solution in the absence of complex. Viscosity values were calculated after correcting the flow time of buffer alone (t_0), $\eta = (t - t_0)/ t_0$ [15].

Cyclic voltammetric and Differential pulse voltammogram studies were performed on a CHI 620C electrochemical analyzer with three electrode system of glassy carbon (GC) as the working electrode, a platinum wire as auxiliary electrode and Ag/AgCl as the reference electrode. All the voltammetric experiments were carried out in single-compartment cells of volume 5-15 mL. Solutions were deoxygenated by purging with N_2 prior to measurements. Increasing amounts of CT DNA were added directly into the cell containing the complex solution (2.5 X 10^{-3} M, 5 mM Tris-HCl/ 50 mM NaCl buffer(pH 7.2). The concentration ranged from 0 to 400 μM for CT DNA. The solution in the cuvette was thoroughly mixed before each scan. All the experiments were carried out at room temperature.

2.4. Chemical nuclease activity

The extent of cleavage of super coiled (SC) pUC19 DNA (33.3 μM, 0.2 μg) to its nicked circular (NC) form was determined by agarose gel electrophoresis in 50 mM Tris–HCl buffer (pH 7.2) containing 50 mM NaCl. The gel electrophoresis experiments were performed by incubation at 37°C for 2 h of 30 μM pUC19 DNA, 50 μM each complex and 50 μM 3-mercaptopropionic acid (MPA) in Tris-HCl buffer (pH 7.2). After incubation, samples were electrophoresed for 2 h at 100 V on 0.8% agarose gel using Tris-acetic acid-EDTA buffer (pH 7.2). The gel was then stained using 1 μg/cm^3 ethidium bromide (EB) and photographed under ultraviolet light at 360 nm. All the experiments were performed at room temperature unless otherwise mentioned.

2.5. Antimicrobial assays

The synthesized ligand and its complexes were tested for their *in vitro* antimicrobial activity against the bacteria *Salmonella typhi, Staphylococcus aureus, Bacillus subtilis, Escherichia coli, Pseudomonas aeruginesa* and *Klebsiella pneumoniae* and fungi *Aspergillus niger, Aspergillus flavus, Rhizopus stolonifer, Candida albicans* and *Rhizoctonia bataicola* by disc diffusion method using potato dextrose agar as medium. The stock solution (10^{-2} mol L^{-1}) was prepared by dissolving the compounds in DMSO and the solutions were serially diluted in order to find the MIC values. In a typical procedure [16], a well was made on the agar medium inoculated with microorganisms. The well was filled with the test solution using a micropipette and the plate was incubated, 24 h for bacteria and 72 h for fungi at 35 °C. During this period, the test solution diffused and the growth of the inoculated microorganisms was affected. The inhibition zone was developed, at which the concentration was noted. Streptomysin and nystatin were used as control drugs.

2.6. Synthesis of Knoevenagel condensate

The nonenolisable diketone was prepared by employing the modified producer reported earlier [17]. Acetylacetone (10 mmol) was stirred with furfuraldehyde (10 mmol) in the presence of 0.2 mL of piperidine for *ca*. 4 h. The reaction mixture was kept at 0 ^{o}C for 48 h. The formed brown solid was washed with an excess of petroleum-ether to remove any unreacted reagents. Washing was repeated two to three times and the compound was recrystallized from $CHCl_3$-petroleum ether mixture to give a pure brown solid, 3-furan-2-ylmethylene-pentane-2,4-dione (Knoevenagel condensate). Yield: 77 %; m.p. 60 ^{o}C. ^{1}H-NMR (in $CDCl_3$): δ 2.1 (s, 6H, CH_3), 8.28 (s, 1H, –C=CH–), 6.5-7.5 (3H, aromatic, furan).

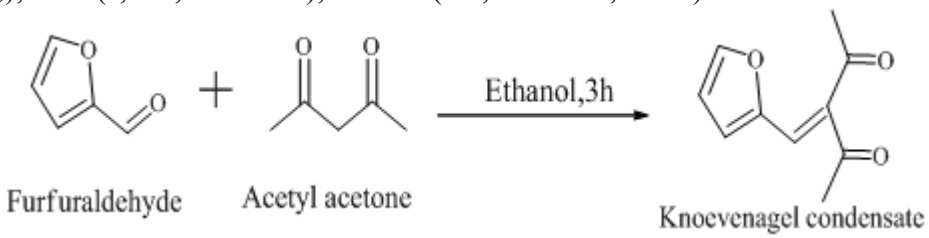

2.7. Synthesis of metal complexes

2.7.1. Synthesis of [M(fmp)$_3$]Cl$_2$

A hot ethanolic solution of Knoevenagel condensate (30 mmol) was stirred with the ethanolic solution of $CoCl_2$/$CuCl_2.2H_2O$ (10 mmol) for *ca.* 2 h and then pH of the reaction mixture was adjusted to 6-7 by the addition of aqueous ammonia. The separated solid complexes were filtered, washed with ethanol and dried in *vacuo*.

2.7.2. Synthesis of [M(fmp)(bpy)$_2$]Cl$_2$ or [M(fmp)(phen)$_2$]Cl$_2$

To a stirred ethanol solution of the Knoevenagel condensate (10 mmol), an ethanolic solution of $CoCl_2$/$CuCl_2.2H_2O$ (10 mmol) was added dropwise. Keeping the reaction at 70 °C for 1 h, a solution of 2,2'-bipyridyl/1,10-phenanthroline (20 mmol) was added. Then, the reaction solution was refluxed for 2 h. The formed solid complexes were filtered, washed with ethanol and dried in *vacuo*.

3. Results and discussion

The synthesized Cu(II) and Co(II) complexes are found to be stable in air. They are only soluble in DMF and DMSO. Physical characterisation, microanalytical, molar conductance and magnetic susceptibility data of the complexes are given in Table.1. The analytical data of the complexes are in good agreement with the formulae [M(fmp)$_3$]Cl$_2$, [M(fmp)(phen)$_2$]Cl$_2$, [M(fmp)(bpy)$_2$]Cl$_2$and [M(fmp)(phen)(bpy)]Cl$_2$; where M=Cu(II) and Co(II). The high conductance of the chelates supports their electrolytic nature.

3.1. Mass spectra

The molecular ion peak for the Knoevenagel condensate is observed at 178 m/z. For copper complex [Cu(fmp)(bpy)(phen)]Cl$_2$, the molecular ion peak, appeared at 649 m/z confirms its stoichiometry (1:1:1:1). An isotopic peak showed at 651 (M+2) m/z proves the presence of two chlorine atoms (Fig. 1) for this complex. Similarly, the mass spectra of other complexes have been recorded and the observed peaks are in good agreement with their empirical formulae as indicated from microanalytical data. Thus, the mass spectral data reinforce the conclusion drawn from the analytical and conductance values.

Table 1
Physical characterization, analytical, molar conductance, and magnetic susceptibility data of the ligand and its complexes

Compound	Color	Yield (%)	Found (Calcd) (%)				Molar Conductance $\wedge_m$(ohm^{-1}cm^2 mol^{-1})	μ_{eff} (BM)
			M	C	H	N		
fmp	Brown	77	----	66.9 (67.4)	5.6 (5.6)	----	----	----
[Cu(fmp)(bpy)(phen)]Cl_2	Blue	48	9.6 (9.8)	58.6 (59.2)	4.0 (4.0)	8.2 (8.6)	132	1.78
[Cu(fmp)(bpy)$_2$]Cl_2	Blue	45	9.9 (10.2)	57.1 (57.6)	4.0 (4.2)	8.6 (8.9)	144	1.71
[Cu(fmp)(phen)$_2$]Cl_2	Blue	54	9.2 (9.4)	60.3 (60.8)	3.9 (3.9)	8.0 (8.3)	138	1.76
[Cu(fmp)$_3$]Cl_2	Greenish blue	55	9.3 (9.5)	53.6 (53.8)	4.5 (4.5)	----	141	1.81
[Co(fmp)(bpy)(phen)]Cl_2	Brown	46	8.8 (9.1)	59.1 (59.6)	4.1 (4.1)	8.3 (8.7)	130	4.23
[Co(fmp)(bpy)$_2$]Cl_2	Brown	50	9.1 (9.5)	57.6 (58.1)	4.2 (4.2)	8.7 (9.0)	126	4.15
[Co(fmp)(phen)$_2$]Cl_2	Brown	42	8.6 (8.8)	60.8 (61.1)	3.9 (3.9)	8.1 (8.4)	142	4.41
[Co(fmp)$_3$]Cl_2	Brown	38	8.6 (8.9)	53.8 (54.2)	4.0 (4.5)	----	139	4.07

3.2. IR spectra

The IR spectra provide valuable information regarding the nature of the functional group attached to the metal atom. IR spectrum of the 3-furan-2-ylmethylene-pentane-2,4-dione exhibits bands around 1675 cm^{-1} (C=C–C=O) and ~2960 cm^{-1} (aromatic =C-H) which are in good agreement with the earlier reports. Lowering of $\gamma_{(C=N)}$ in the complexes (1600-1609 cm^{-1}) as compared to 1,10-phenanthroline and 2,2'-bipyridine (1630 cm^{-1}) [18] is due to reduction of double bond character of carbon-nitrogen bond. This indicates that the metal ion is coordinated by the nitrogen atoms of 1,10-phenanthroline [19] and 2,2'-bipyridine. A strong band observed at 1675 cm^{-1} in 3-furan-2-ylmethylene-pentane-2,4-dione corresponding to $\gamma_{(C=O)}$ of acetylacetone moiety is shifted to lower frequencies (1635-1654 cm^{-1}), which indicates the coordination of the carbonyl oxygen with metal ion. Assignment of the proposed coordination sites is further supported by the appearance of medium bands at 450-400 cm^{-1} which could be attributed to ν_{M-N} [20].

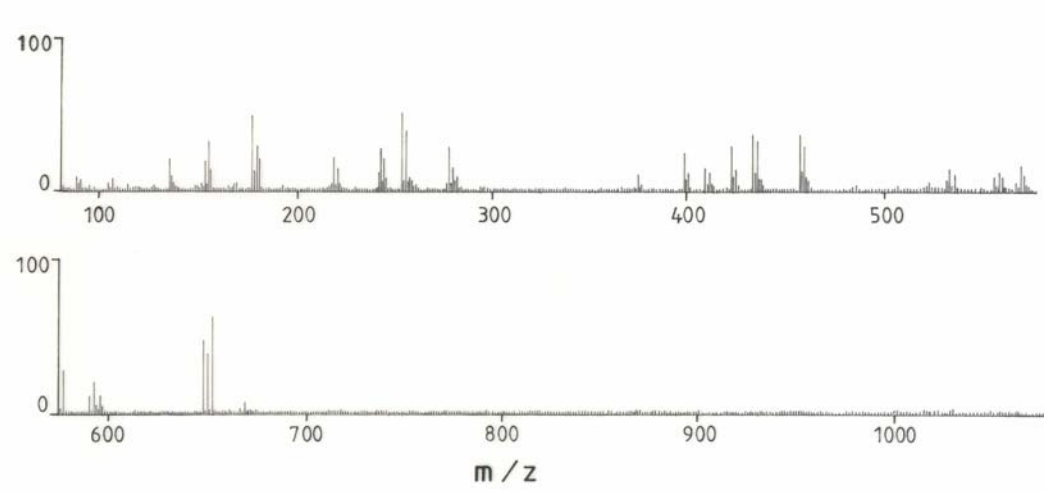

Fig. 1. The mass spectrum of $[Cu(fmp)(bpy)(phen)]Cl_2$

3.3 Electronic absorption spectra

The electronic absorption spectra of 3-furan-2-ylmethylene-pentane-2,4-dione and its Cu(II) and Co(II) complexes are recorded at room temperature using DMF as the solvent. The absorptions shown by 3-furan-2-ylmethylene-pentane-2,4-dione at 41493, 34246 and 32362 cm^{-1} are intra-ligand charge transfer transitions, assigned to $n–\pi^*$ (41493 cm^{-1}) transition of the carbonyl groups and $\pi–\pi^*$ transitions (34246 and 34246 cm^{-1}) [21, 22]. The four synthesized Cu(II) complexes, $[Cu(fmp)(bpy)(phen)]Cl_2$, $[Cu(fmp)(bpy)_2]Cl_2$, $[Cu(fmp)(phen)_2]Cl_2$ and $[Cu(fmp)_3]Cl_2$ show broad bands at 13510, 13420, 13380 and 13,350 cm^{-1} respectively assigned to the $^2E_g \rightarrow {}^2T_{2g}$ transition [23, 24].

Also these Cu(II) complexes show shoulder at 26666, 26385, 26954 and 27110 cm^{-1} respectively which correspond to intra-ligand charge transfer transitions. The observed results said that the four Cu(II) complexes are having distorted octahedral geometry. The four Co(II) complexes, $[Co(fmp)(bpy)(phen)]Cl_2$, $[Co(fmp)(bpy)_2]Cl_2$, $[Co(fmp)(phen)_2]Cl_2$ and $[Co(fmp)_3]Cl_2$ show broad bands at 17120, 17165, 17090 and 17150 cm^{-1} respectively, assigned to the $^4T_{1g}(F) \rightarrow {}^4A_{2g}(F)$ transition [25]. Also the Co(II) complexes show shoulder at 28740, 28490, 29910 and 28870 cm^{-1} respectively which correspond to intra-ligand charge transfer transitions. The observed results said that the four Co(II) complexes are having octahedral geometry.

3.4. Electron Spin Resonance Spectrum

The ESR spectrum of the complex, $[Cu(fmp)(bpy)(phen)]Cl_2$ at 300 K shows one intense absorption band in the high field region and is isotropic due to dumpling motion of the molecules (Fig. 2). The magnetic moment calculated from the equation $\mu_{eff} = g[s(s+1)]^{1/2}$ using the experimental g_{iso} values(2.23) agree very well with the measured magnetic susceptibility range of 1.73–2.02 B.M indicating that the solid structure is retained in DMSO solution. The ESR spectrum of the copper complex at 77 K indicates a poorly resolved nitrogen super hyperfine structure (Fig. 3) in the perpendicular region due to the interaction of the Cu(II) odd electron with nitrogen atoms. The magnetic susceptibility value reveals that the copper complex has a magnetic moment, 1.78 BM, corresponding to the one unpaired electron, indicating that the complex is mononuclear. This fact was also evident from the absence of a half field signal,

observed in the spectrum at 1800 G due to the $m_s = \pm 2$ transitions, ruling out any Cu-Cu interaction.

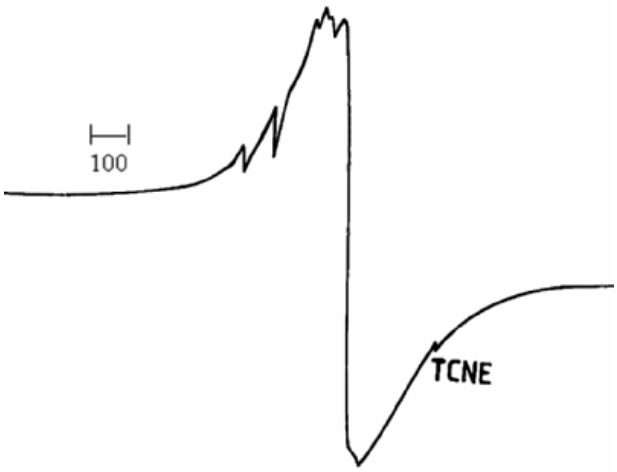

Fig. 2. The ESR spectrum of $[CuL(phen)(bpy)]Cl_2$ complex at 300 K in DMSO solution

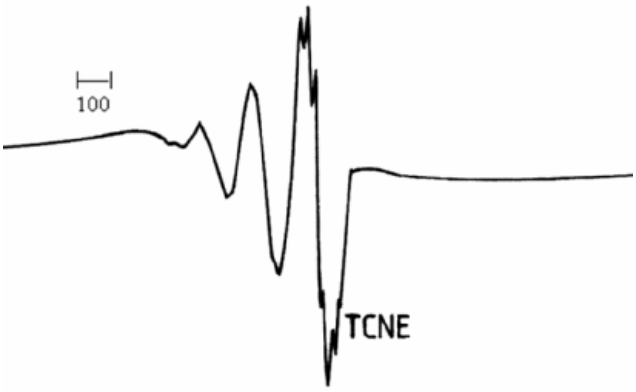

Fig. 3. The ESR spectrum of $[CuL(phen)(bpy)]Cl_2$ complex 77 K in DMSO solution

The observed A_{II}, $A_{\perp}$, g_{II} and $g_{\perp}$ values are 125.7 G, 58 G, 2.23 and 2.05 respectively. The g tensor values of this copper(II) complex can be used to derive the ground state. In octahedral complexes, the unpaired electron lies in the $d_{x^2-y^2}$ orbital giving $g_{II} > g_{\perp} > 2$. From the observed values, it is clear that $g_{II} > g_{\perp} > 2$ which suggests that the complex is octahedral. Further, this is also supported by the fact that the unpaired electron lies predominantly in the $d_{x^2-y^2}$ orbital [26], as was evident from the value of the exchange interaction term G, estimated from the expr

$$G = (g_{II}-2-0023) / (g_{\perp}-2.0023)$$

Kivelson and Nielson [27] Pointed out that g_{II} value for Cu(II) complexes are moderately sensitive function of metal-ligand covalency. For ionic environments g_{II} is normally 2.3 or larger and for more covalent environment, it is less than 2.3. The observed g_{II} value is 2.23 which is an indication of a strong covalent environment in the Cu(II) complex.

If G > 4.0, the local tetragonal axes are aligned parallel or only slightly misaligned. If G < 4.0, significant exchange coupling is present and the misalignment is appreciable. The observed value for the exchange interaction parameter for the copper complex (G =4.77) suggests that the local tetragonal axes are aligned parallel or slightly misaligned, and the unpaired electron is present in the $d_{x^2-y^2}$ orbital. This result also indicates that the present copper complex having G value of 4.77 suggests that the local tetragonal axes are aligned parallel or slightly misaligned and are consistent with a $d_{x^2-y^2}$ ground state. Based on the spectral data, the structure of the complex is given in Fig. 4.

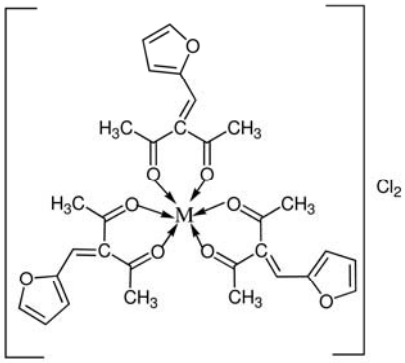

Fig. 4a. Structure of $[M(fmp)_3]Cl_2$

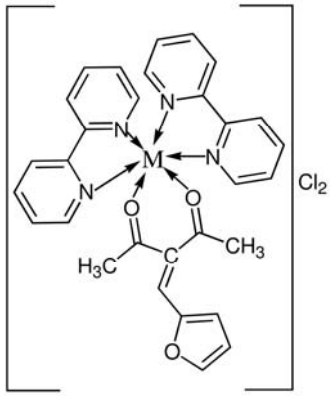

Fig. 4b. Structure of $[M(fmp)(bpy)_2]Cl_2$

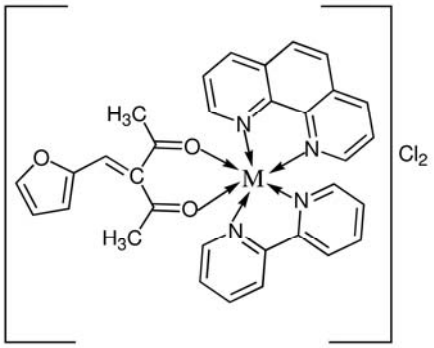

Fig. 4c. Structure of $[M(fmp)_3(bpy)(phen)]Cl_2$

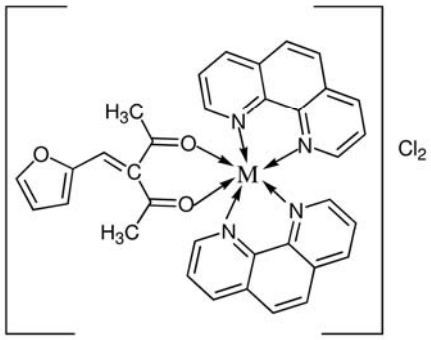

Fig. 4d. Structure of $[M(fmp)(phen)_2]Cl_2$

M = Co(II) or Cu(II)

3.5. DNA binding studies

3.5.1. Electronic spectra

Absorption titration is used to monitor the interaction of the complexes with CT DNA. In general, a complex bound to DNA through intercalation usually results in hypochromism and red shift (bathochromism) of the absorption band due to strong stacking interaction between aromatic chromophore of the complex and the base pairs of the DNA. Intense absorption bands are observed for synthesized complexes from 285–390 nm which are attributed to the LMCT transition involving the heterocyclic base and the metal ion. On increasing the CT-DNA concentration, the hypochromism is found to increase with a red shift in the UV band of the

complexes. In order to compare the binding strength of the complexes with CT DNA, the intrinsic binding constants K_b are obtained by monitoring the changes in absorbance for the complexes with increasing concentration of DNA. K_b is obtained from the ratio of slope to the intercept from the plots of [DNA]/($(\varepsilon_a-\varepsilon_f)$ *versus* [DNA]. The K_b values are in the order of 10^5, 10^4 and 10^3 M^{-1} for the $[M(fmp)(phen)_2]Cl_2$, $[M(fmp)(phen)(bpy)]Cl_2$ and $[M(fmp)(bpy)_2]Cl_2$ complexes, respectively (Table 2). The high K_b value for the $[M(fmp)(phen)_2]Cl_2$ complexes in comparison to their bpy analogue is possibly due to the presence of extended planar structure of the phen ligand greatly facilitating groove binding/stacking with the base pairs. The $[M(fmp)_3]Cl_2$ complex in absence of any planar moiety does not show any apparent binding to DNA (Fig. 5).

Table 2
Absorption spectral properties of synthesized complexes with CT DNA.

SI.No	Complexes	λmax		Δλ (nm)	H%	K_b (M^{-1})
		Free	Bound			
1	$[Co(fmp)_3]Cl_2$	285.3	286.0	0.7	2.4	1.8×10^1
2	$[Cu(fmp)_3]Cl_2$	314.6	315.2	0.6	2.7	2.3×10^1
3	$[Co(fmp)(bpy)_2]Cl_2$	336.3	337.9	1.6	5.1	3.4×10^3
4	$[Cu(fmp)(bpy)_2]Cl_2$	330.2	331.5	1.3	5.5	4.2×10^3
5	$[Co(fmp)(bpy)(phen)]Cl_2$	351.5	354.5	2.0	8.5	2.6×10^4
6	$[Cu(fmp)(bpy)(phen)]Cl_2$	354.8	356.8	2.0	9.2	3.4×10^4
7	$[Co(fmp)(phen)_2]Cl_2$	382.4	385.6	3.2	12.4	4.6×10^5
8	$[Cu(fmp)(phen)_2]Cl_2$	386.5	390.0	3.5	13.5	5.8×10^5

3.5.2. Redox chemistry

Typical CV curves for 5×10^{-3} mol dm^{-3} of $[CuL(phen)(bpy)]Cl_2$ in Tris-HCl buffer (pH 7.2) in the absence and presence of different concentration of DNA are shown in Fig. 6. The electrochemical data are given in Table 3. All the copper complexes show one well-defined redox couple corresponding to copper(II)/(I), as expected. In the absence of DNA cathodic peak appears in the range of 0.140 –0.525 V corresponds to the one electron reduction of copper(II) and the corresponding anodic peak appears in the 0.408–0.630 mV positive potential region. The measured ΔEp values (0.125-0.132 V) clearly indicate that these redox couples are quasi-reversible. The ipa/ipc falls at less than unity, clearly confirming one electron transfer in this redox process. The incremental addition of CT DNA to the complex the redox couples causes a negative shift in $E_{1/2}$ and a decrease in ΔEp. The ip_c/ip_a values also decrease in the presence of DNA. The decrease of the anodic and cathodic peak currents of the complex in the presence of DNA is due to decrease in the apparent diffusion coefficient of the copper(II) complex upon complexation with the DNA macromolecule. These results show that copper(II) complex stabilizes the duplex (GC pairs) by intercalating way.

In the absence of CT DNA, the first redox couple cathodic peak appears in the region of 0.050–0.140 V for Co(III) → Co(II). The measured ΔEp (0.080–0.140 V) and ipa/ipc (less than unity) is clearly indicates that these redox couples are quasi-reversible. The second redox couple cathodic peak appears in the range of -0.082 to -0.14 V for Co(II) → Co(I). The observed range of ΔEp (0.246–0.381 V) and ipa/ipc (less than unity) indicates that the reaction of the complex on GC electrode surface is quasi-reversible redox process. The incremental addition of CT DNA to the complex, the first redox couple causes a negative shift in $E_{1/2}$ and a decrease in ΔEp. The ip_c/ip_a values also decrease in the presence of DNA. The decrease of the anodic and cathodic peak currents of the complexes in the presence of DNA is due to decrease in the apparent diffusion coefficient of the cobalt(II) complexes upon complexation with the DNA

macromolecules. But, the second redox couple of cobalt(II) complex shows no significant change of potential as well as intensity of current. This indicates that the second redox couple species does not stabilize the duplex DNA.

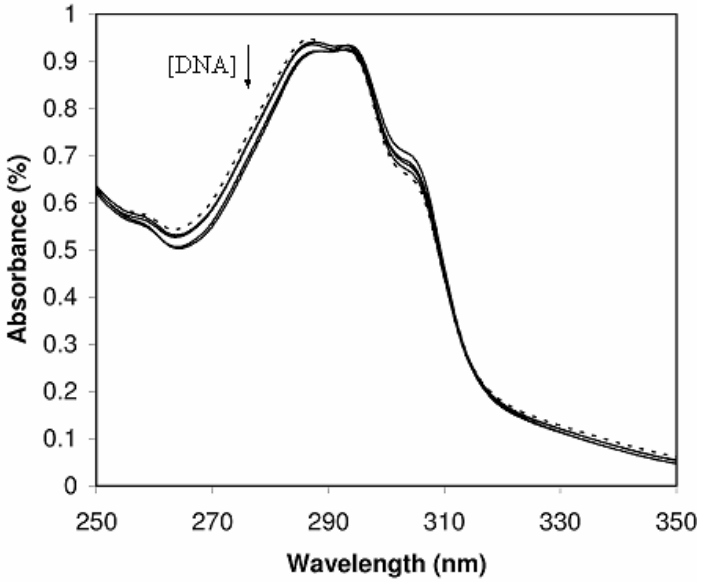

Fig. 5. Electronic absorption spectra of $[Co(fmp)_3]Cl_2$ in the absence (dash line) and presence (dark line) of increasing amounts of DNA.

Table 3
Electrochemical parameters for the interaction of DNA with Co(II) and Cu(II) complexes.

SI. No	Complexes	Redox couple	$E_{1/2}$ (V)		ΔEp (V)		k[red]/ k[oxd]	Ipc/Ipa
			Free	Bound	Free	Bound		
1	$[Co(fmp)_3]Cl_2$	Co(III)/Co(II)	0.087	0.072	0.063	0.069	0.94	0.86
2	$[Cu(fmp)_3]Cl_2$	Cu(II)/Cu(I)	0.564	0.568	0.125	0.092	0.94	0.98
3	$[Co(fmp)(bpy)_2]Cl_2$	Co(III)/Co(II)	0.082	0.075	0.070	0.075	0.85	0.82
4	$[Cu(fmp)(bpy)_2]Cl_2$	Cu(II)/Cu(I)	0.285	0.277	0.294	0.262	0.87	0.91
5	$[Co(fmp)(bpy)(phen)]Cl_2$	Co(III)/Co(II)	0.149	0.137	0.025	0.018	0.89	0.99
6	$[Cu(fmp)(bpy)(phen)]Cl_2$	Cu(II)/Cu(I)	0.336	0.324	0.312	0.301	0.93	0.88
7	$[Co(fmp)(phen)_2]Cl_2$	Co(III)/Co(II)	0.138	0.155	0.068	0.049	0.78	0.89
8	$[Cu(fmp)(phen)_2]Cl_2$	Cu(II)/Cu(I)	0.486	0.464	0.216	0.195	0.84	0.96

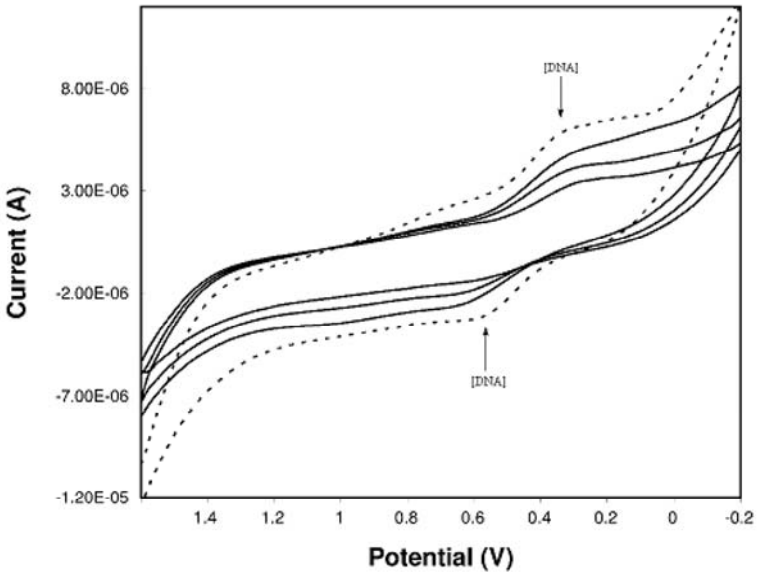

Fig. 6. Cyclic voltammograms of $[Cu(fmp)(phen)_2]Cl_2$ in the absence (dotted line) and presence of (dark line) of DNA

3.5.3. Differential pulse voltammogram study

Differential pulse voltammogram curves for 5×10^{-3} mol dm^{-3} of the $[Cu(fmp)(phen)_2]Cl_2$ in Tris-HCl buffer (pH 7.2) both in the absence and presence of varying amount of DNA are shown in Fig. 7.

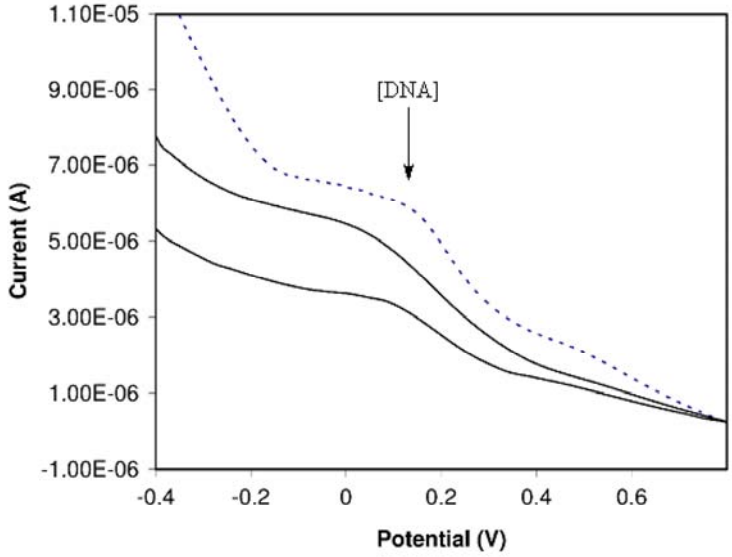

Fig. 7. Differential pulse voltammograms of the $[Cu(fmp)(phen)_2]Cl_2$ in the absence (dotted line) and presence (dark line) of DNA.

The peak potential and current intensity of the Cu(II) and Co(II) complexes are changed in the presence of DNA. According to the equation,

$$E_b - E_f = 0.0591 \log (K_{[red]}/K_{[oxd]})$$

where E_b and E_f were formal potential of the Cu(II)/Cu(I) complex or Co(III)/Co(II) couple in the bound and free forms, respectively. The ratio of the binding constants ($K_{[red]}/K_{[oxd]}$) for DNA binding of the Cu(II)/Cu(I) and Co(III)/Co(II) couples of the complexes has been found to be less than unity. These results indicate that copper and cobalt in +2 oxidation form bind to DNA more efficiently than the +1 and +3 oxidation forms of copper and cobalt complexes respectively.

3.5.4. Viscosity studies

Furthermore, the interactions between the complexes and DNA have been investigated by viscosity measurements. Optical photophysical probes provided necessary, but not sufficient clues to support a binding model. Hydrodynamic measurements that are sensitive to length change (i.e., viscosity and sedimentation) are regarded as the least ambiguous and the most critical tests of binding mode in solution in the absence of crystallographic structural data [28]. A classical intercalation model usually results in lengthening the DNA helix, as base pairs are separated to accommodate the binding ligand leading to the increase of DNA viscosity. As seen in Fig. 8, $[M(fmp)_3]Cl_2$ actually has no effect of viscosity which indicates that $[M(fmp)_3]Cl_2$ is not bound to DNA. But viscosity of CT DNA for other complexes increases significantly as increasing the concentration of the complexes. However, $[M(fmp)(phen)_2]Cl_2$ shows more effective changes in the viscosity of DNA due to extending the planarity of the complex so that the binding affinity of DNA is high. These results also parallel to the above spectroscopic results, such as hypochromism, red-shift of complexes in the presence of DNA.

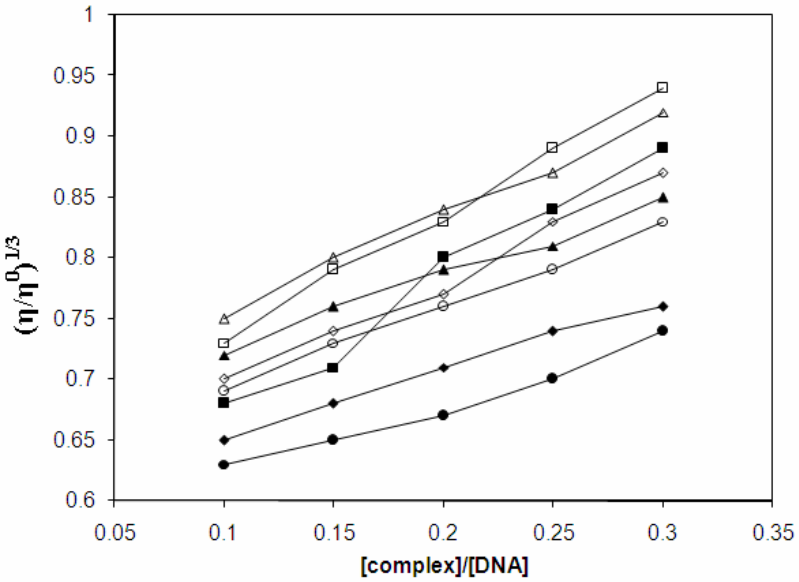

Fig. 8. The effect of $[Co(fmp)_3]Cl_2$ (●), $[Cu(fmp)_3]Cl_2$ (♦), $[Co(fmp)(bpy)_2]Cl_2$ (○), $[Cu(fmp)(bpy)_2]Cl_2$ (◇), $[Co(fmp)(bpy)(phen)]Cl_2$ (▲), $[Cu(fmp)(bpy)(phen)]Cl_2$ (■), $[Co(fmp)(phen)_2]Cl_2$ (△) and $[Cu(fmp)(phen)_2]Cl_2$ (□) on the viscosity of DNA; Relative specific viscosity *versus* R = [Complex] / [DNA].

3.6. DNA Cleavage studies

The DNA cleavage efficiency of the complexes compared to that of the control is due to their efficient DNA–binding ability. The metal complexes are able to convert super coiled DNA (Form-I) into open circular DNA (Form-II). The proposed general oxidative mechanisms account the DNA cleavage by hydroxyl radicals *via* abstraction of a hydrogen atom from sugar

units and predict the release of specific residues arising from transformed sugars, depending on the position from which the hydrogen atom is removed. The cleavage is inhibited by the free radical scavengers implying that hydroxyl radical or peroxy derivatives mediate the cleavage reaction. The reaction is modulated by a metallo-complex bound hydroxyl radical or a peroxo species generated from the co-reactant 3-mercaptopropionic acid (MPA).

In the present study, the pUC19 DNA gel electrophoresis experiment is conducted at 35°C using the synthesized complexes in the presence of MPA as reducing agent. As can be seen from the results in Fig. 9, control experiments using $[M(fmp)_3]Cl_2$ do not show any significant cleavage of pUC19 DNA even on longer exposure time. Hence, binding of $[M(fmp)_3]Cl_2$ with DNA is inactive. $[M(fmp)(phen)_2]Cl_2$ shows more cleavage activity compared to other complexes. This result suggests that $[M(fmp)(phen)_2]Cl_2$ has more binding ability with DNA. The DNA cleavage activity order of the complexes as follows: $[M(fmp)_3]Cl_2$ < $[M(fmp)(bpy)_2]Cl_2$ < $[M(fmp)(bpy)(phen)]Cl_2$ < $[M(fmp)(phen)_2]Cl_2$. From this order, it is observed that planarity of the complexes increases the binding and cleavage activities of the complexes.

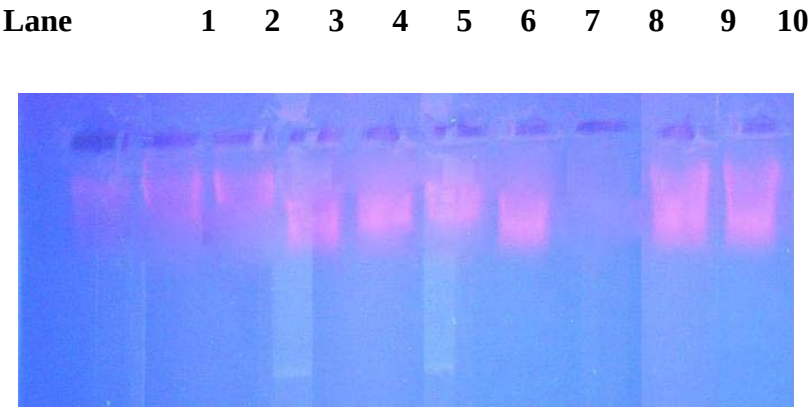

Fig. 9. Gel electrophoresis diagram showing DNA cleavage of pUC19 DNA (30 μm) by synthesized compounds in ethanol/DMF in the presence of MPA (50 μm) in a Tris-HCl buffer (pH 7.2) at 37° C. lane 1, DNA Control; lane 2, DNA + $[Co(fmp)_3)]Cl_2$ + MPA; lane 3, DNA + $[Cu(fmp)_3)]Cl_2$ + MPA; lane 4, DNA + $[Co(fmp)(bpy)_2)]Cl_2$ + MPA; lane 5, DNA + $[Cu(fmp)(bpy)_2)]Cl_2$ + MPA; lane 6, DNA + $[Co(fmp)(bpy)(phen)]Cl_2$ + MPA; lane 7, DNA + $[Cu(fmp)(bpy)(phen)]Cl_2$ + MPA; lane 8, DNA + ligand + MPA; lane 9, DNA + $[Co(fmp)(phen)_2]Cl_2$ + MPA; lane 10, DNA + $[Cu(fmp)(phen)_2]Cl_2$ + MPA

3.7. Antimicrobial assay

The bacteria *Salmonella typhi, Staphylococcus aureus, Bacillus subtilis, Escherichia coli, Pseudomonas aeruginesa* and *Klebsiella pneumoniae* and fungi *Aspergillus niger, Aspergillus flavus, Rhizopus stolonifer, Candida albicans* and *Rhizoctonia bataicola* are selected to test the *in vitro* antimicrobial activity of the investigated compounds. Tables 4 and 5 summarize the minimum inhibitory concentration (MIC) values of the investigated compounds. It is clear from the tables that the observed MIC values indicate that most of the complexes have higher antimicrobial activity than the free ligand, fmp. Such increased activity of the metal chelates can be explained on the basis of chelation theory [29]. On chelation, the polarity of the metal ion will be reduced to a greater extent due to the overlap of the ligand orbital and partial sharing of the positive charge of the metal ion with donor groups. Further, it increases the delocalization of π-electrons over the whole chelate ring and enhances the penetration of the complexes into lipid membranes and blocking of the metal binding sites in the enzymes of microorganisms. These

complexes also disturb the respiration process of the cell and thus block the synthesis of proteins, which restricts further growth of the organisms [30].

Table 4
Minimum inhibition concentration of the synthesized compounds against the growth of six bacteria (mg/mL)

S.No	Compound	*S. typhi*	*S. aureus*	*B. subtilis*	*E. coli*	*P. aeruginosa*	*K. pneumoniae*
1	fmp	65	80	70	85	75	70
2	$[Cu(fmp)(bpy)(phen)]Cl_2$	22	28	42	20	38	32
3	$[Cu(fmp)(bpy)_2]Cl_2$	26	30	45	28	44	40
4	$[Cu(fmp)(phen)_2]Cl_2$	20	24	36	18	30	26
5	$[Cu(fmp)_3]Cl_2$	30	34	48	32	48	44
6	$[Co(fmp)(bpy)(phen)]Cl_2$	24	34	46	30	42	34
7	$[Co(fmp)(bpy)_2]Cl_2$	28	38	50	38	46	40
8	$[Co(fmp)(phen)_2]Cl_2$	22	28	40	25	36	30
9	$[Co(fmp)_3]Cl_2$	34	40	55	48	54	50
10	Streptomycin	18	12	10	14	18	12

Table 5
Minimum inhibition concentration of the synthesized compounds against the growth of five fungi (mg/mL)

S.No	Compound	*A. niger*	*A. flavus*	*R. stolonifer*	*C. albicans*	*R. bataicola*
1	fmp	75	80	85	75	70
2	$[Cu(fmp)(bpy)(phen)]Cl_2$	40	38	42	26	34
3	$[Cu(fmp)(bpy)_2]Cl_2$	48	30	44	35	28
4	$[Cu(fmp)(phen)_2]Cl_2$	24	22	34	20	25
5	$[Cu(fmp)_3]Cl_2$	50	48	52	32	36
6	$[Co(fmp)(bpy)(phen)]Cl_2$	42	45	48	36	38
7	$[Co(fmp)(bpy)_2]Cl_2$	46	52	54	42	34
8	$[Co(fmp)(phen)_2]Cl_2$	28	38	40	30	28
9	$[Co(fmp)_3]Cl_2$	56	54	60	35	42
10	Nystatin	10	8	16	12	14

4. Conclusions

The analytical and spectral data reveal that the synthesized complexes exhibit octahedral geometry around the central metal ions. The intercalative binding of the complexes with the DNA has been supported by electronic absorption spectra, cyclic voltammetry, difference pulse voltammetry and viscometric studies. The planarity of the complexes increases the DNA binding and cleavage activities. The results obtained from *in vitro* antifungal and antibacterial tests together show that all the complexes are much potent activities towards bacteria and fungi. It has been found that the activities of the complexes are higher than the free ligand.

Acknowledgements

The authors express their sincere thanks to the Principal, Head of the Department of Chemistry and the College Managing Board, VHNSN College for providing the research facilities. NR and RJ express their gratitude to the Department of Science and Technology, New Delhi for the financial assistance.

References

[1] R.N. Prasad, M. Agarwal, S. Sharma, Indian J. Chem. 43A (2004) 337-340.
[2] N.K. Singh, S.K. Kushawaha, Indian J. Chem. 43A (2004) 333-336.
[3] N. Raman, V. Muthuraj, S. Ravichandran, A. Kulandaisamy, Proc. Indian Acad. Sci. 115 (2003) 161-167.
[4] A.V. Ablov, Russ. J. Inorg. Chem. 6 (1961) 157-161.
[5] S. Brini, R. Bucci, V. Carunchio, G. Grassinistrazza, J. Coord. Chem. 17 (1988) 221-226.
[6] E. Casassas, A. Izquierdo-Ridora, R. Tauler, J. Chem. Soc., Dalton Trans. (1990) 2341-2345.
[7] W.R. Mc Whinnie, J. Chem. Soc. (1964) 5165-5169.
[8] R.R. Osborne, W.R. Mc Whinnie, J. Chem. Soc. (1967) 2075-2078.
[9] D.P. Segers, M.K. De Armond, J. Phy. Chem. 86 (1982) 3768-3776.
[10] A. Sengul, Turk. J. Chem. 28 (2004) 703-713.
[11] D.D. Perrin, W.L.F. Armarego, D.R. Perrin, Purification of Laboratory Chemicals, Pergamon Press, Oxford, 1980.
[12] J. Marmur J. Mol. Biol. 3 (1961) 208-218.
[13] M.E. Reichmann, S.A. Rice, C.A. Thomas, P. Doty, J. Am. Chem. Soc. 76 (1954) 3047-3053.
[14] B. Charies, N. Dattagupta, D.M. Crothers, Biochemistry, 21 (1982) 3933-3937.
[15] S. Satyanarayana, J.C. Daborusak, J.B. Charies, Biochemistry, 32 (1983) 2573-2584.
[16] M.J. Pelzar, E.C.S. Chan, N.R. Krieg, Antibiotics and Other Chemotherapeutic Agents, in Mirobiology, 5th Edn., Blackwell Science: New York, 1998.
[17] M. Yamashita,Y. Watanabe,T-a. Mitsudo, Y. Takegami, Bull. Chem. Soc, Jpn. 51 (1978) 835-838.
[18] N. Ren, J-J. Zhang, S-L. Xu, R-F. Wang, S-P. Wang, Thermochim. Acta, 438 (2005) 172-177.
[19] J.J. Zhang, N. Ren, Y.X. Wang, S.L. Xu, R.F. Wang, S.P. Wang, J. Braz. Chem. Soc. 17 (2006) 1355-1359.
[20] M. Thomas, M.K.M. Nair, K. Radhakrishnan, Synth. React. Inorg. Met.-Org. Chem. 25 (1995) 471-479.
[21] C. Spinu, M. Pleniceanu, C. Tigae, Turk. J. Chem. 32 (2008) 487-493.
[22] S. Akine, T. Taniguchi, T. Nabeshima, Inorg. Chem. 43 (2004) 6142-6144.
[23] C.R. Saha, S.K. Hoga, Indian J. Chem. (1986) 340-345.
[24] Y. Prasanthi, K. Kiranmai, N.J.P. Subhashini, Shivaraj, Spectrochim. Acta, 70A (2008) 30-35.
[25] F. Firdaus, K. Fatma, M. Azam, S.N. Khan, A.U. Khan, M. Shakir, Transition Met. Chem. 33 (2008) 467-473.
[26] R.M. Kadam, M.D. Sastry, M.K. Bhide, S.A. Chavan, J.V. Yakhmi, O. Khan, Chem. Phys. Lett. 281 (1997) 292-296.
[27] K. Jeyasubramanian, S.A. Samath, S. Thambidurai, R. Murugesan, S.K. Ramalingam, Transition Met. Chem. 20 (1996) 76-80.
[28] B.C. Baguley, M. Lebret, Biochemistry, 23 (1984) 937-943.
[29] N. Dharmaraj, P. Viswanathamurthi, K. Natarajan, Transition Met. Chem. 26 (2001) 105-109.
[30] A. Kriza, A. Reiss, S. Florea, T. Caproiu, J. Indian Chem. Soc. 77 (2000) 207-208.